Available online at www.sciencedirect.com
SCIENCE DIRECT®
Journal of Theoretical Biology 233 (2005) 253–269
Journal of Theoretical Biology
www.elsevier.com/locate/yjtbi

Formation of the chick primitive streak as studied in computer simulations

L. Bodenstein[a,*], C.D. Stern[b]

[a]Olana Technologies Inc.,5424 Arlington Avenue, H51, Bronx, NY 10471 USA
[b]Department of Anatomy and Developmental Biology, University College London, Gower Street, London WC1E 6Bt UK

Received 31 May 2004; received in revised form 6 October 2004; accepted 8 October 2004

Abstract

We have used a computer simulation system to examine formation of the chick primitive streak and to test the proposal (Wei and Mikawa Development 127 (2000) 87) that oriented cell division could account for primitive streak elongation. We find that this proposal is inadequate to explain elongation of the streak. In contrast, a correctly patterned model streak can be generated if two putative mechanisms are operative. First, a subpopulation of precursor cells that is known to contribute to the streak is assigned a specific, but simple, movement pattern. Second, additional cells within the epiblast are allowed to incorporate into the streak based on near-neighbor relations. In this model, the streak is cast as a steady-state system with continuous recruitment of neighboring epiblast cells, egress of cells into deeper layers and an internal pattern of cell movement. The model accurately portrays elongation and maintenance of a robust streak, changes in the composition of the streak and defects in the streak after experimental manipulation.

Keywords: Morphologenesis; Chick primitive streak; Computer simulations

1. Introduction

Formation of the primitive streak is the most important event of gastrulation in amniote (reptile, avian and mammalian) embryos. The primitive streak arises from the posterior pole of the epiblast and elongates rapidly in an anterior direction until it reaches to just beyond the center of the embryo (Fig. 1). This occurs between embryonic stage XIV and stage 3+ (Hamburger and Hamilton, 1951; Eyal-Giladi and Kochav, 1976), a period of about 9 h (Spratt, 1946). Indeed, most of this rapid elongation can be seen by cine analysis to occur over as brief a time as 3–6 h (Foley et al., 2000). Although the streak eventually regresses, it forms the essential conduit for gastrulation and serves to define the anteroposterior axis of the embryo.

Formation of the streak may involve: (i) a visible change, conformational or compositional, in *in situ* cells, (ii) new cells taking up residence in the region of the evolving streak, or (iii) a combination of these mechanisms. The speed with which the streak evolves suggests the first possibility, but careful marking experiments (Eyal-Giladi et al., 1992; Bachvarova et al., 1998; Wei and Mikawa, 2000; Lawson and Schoenwolf, 2001b) have demonstrated that cells throughout the evolving streak are derived from *Koller's sickle* (an arc of cells at the posterior edge of the epiblast—see Appendix A) and the neighboring epiblast (here termed, *sickle-associated epiblast*). Cells that contribute to the primitive streak are located at the extreme posterior margin of the epiblast prior to streak formation and then are rapidly dispersed along the posterior midline.

The mechanisms that distribute these cells and result in formation of the streak are largely unknown. It has been suggested that elongation of the primitive streak is

*Corresponding author.
E-mail address: lb@olana-tech.com (L. Bodenstein).

0022-5193/$ - see front matter © 2004 Elsevier Ltd. All rights reserved.
doi:10.1016/j.jtbi.2004.10.008

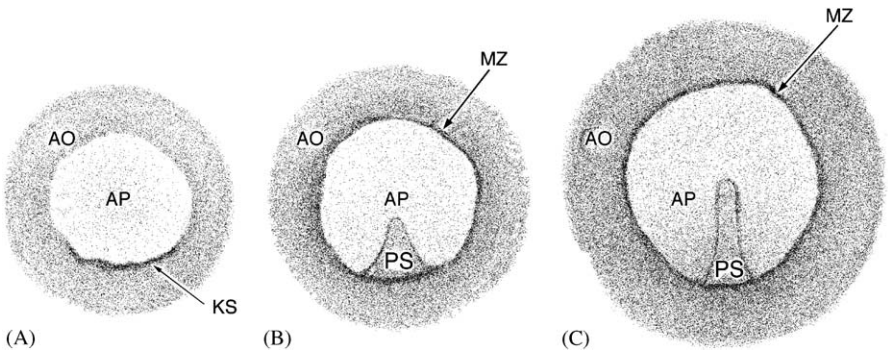

Fig. 1. Shown are representations of the dorsal surface of the chick embryo at (A) stage XIII, (B) stage 2, and (C) stage 3+. AO—area opaca, AP—area pellucida, MZ—marginal zone, KS—Koller's sickle, PS—primitive streak (after Patten, 1971).

driven by oriented cell division within this cell population (Wei and Mikawa, 2000). Here, we use a computer simulation model to distinguish this possibility from an alternative—directed migration and near-neighbor recruitment.

2. Simulations

All simulations were performed using the *Nudge*++ modeling system. Details of the modeling system and its application to the primitive streak are provided in Appendix B. In brief, cells are modeled as inelastic spheres confined to a disc. They carry out individual cellular programs and the model tissue evolves as the pooled behavior of these individual cells. Simulations are generated by specifying the individual cellular programs and observing the generated tissue patterns. Simulations are summarized in Table 1 and described in detail below.

Our interest here is elongation of the primitive streak as occurs between stage XIV and stage 3+ (Fig. 1), although some simulations have been run to later stages as needed. Preceding and contemporaneous with streak formation, the entire epiblast is engaged in a large-scale pattern of cell movements (Figs. 2 and 3; see Appendix A). Here, we distinguish this pattern of global movements from the specific actions that result in primitive streak formation, the latter being much more focused in both time and space and, we infer, differently arranged in the embryo. However, since primitive streak choreography is performed on this moving stage, we begin our simulations with these global movements and maintain them as background through all subsequent simulations.

Our simulations include a stochastic component and each simulation has been run at least ten times. Examples shown were then chosen to reflect the range of possible outcomes:

2.1. Background movements

To recreate the experimentally defined global movement pattern (see Appendix A; Gräper, 1929; Wetzel, 1929; Spratt, 1946; Eyal-Giladi et al., 1992; Hatada and Stern, 1994; Levy and Khaner, 1998; Foley et al., 2000; Lawson and Schoenwolf, 2001b; rev. Romanoff, 1960) cells throughout the epiblast were instructed to move in a position-dependent fashion that was designed to match the experimental data.

These movements produce a general elongation and relative narrowing of the posterior epiblast as seen in the embryo (Fig. 4). In general, cells are driven toward the posterior epiblast where they amass and force the characteristic elongation. The degree of elongation is an increasing function of the rate of cell movement relative to the mitotic rate (not shown).

This global pattern is maintained as a constant background program for all further simulations.

2.2. Focus on the streak

For simulations of the streak itself, we have highlighted a small cohort of cells in the posterior epiblast (designed to represent the streak precursors of Koller's sickle and the sickle-associated epiblast) of the initial (stage XIII) tissue (Fig. 5a). We have followed these precursors and their progeny as the model tissue progresses to the 12 h time point (about Stage 3+). Note that the background cell movement pattern (without any streak-specific component) causes these cells to become distributed along the posterior midline in a pattern reminiscent of the streak (Fig. 5b).[1]

[1]The global movement pattern includes a circumferential component laterally and an "updraft" from posterior to anterior in the posterior midline (see Appendix A). Clearly, this updraft will tend to distribute posterior cells to more anterior positions and thus foreshadow streak formation. However, these global movements, including the updraft, begin many hours in advance of streak formation. The updraft appears to be incidental to streak formation, although it may serve to position

Table 1
Shown is a summary table of the simulations produced in this study

Simulation	Procedures	Major results	Fig.	Related experimental work
Background movement pattern (BMP)	Circumferential movement of cells with "updraft" in posterior midline	Elongation of posterior epiblast; partial distribution of extreme posterior cells along posterior midline	4, 5b	Spratt (1946), Foley et al., 2000
BMP + Oriented cell division in streak	Background movement for all cells; streak cells divide with anteroposterior orientation	Minimal elongation of streak over background effects	6	Wei and Mikawa (2000)
BMP + Directed cell movement in streak (DCM)	Background movement for all cells; streak cells add anteriorly directed movement	Adequate elongation of streak but it is sparsely populated	7	Bachvarova et al. (1998), Wei and Mikawa (2000), Lawson and Schoenwolf (2001a, b)
BMP + DCM + Recruitment of neighboring cells to streak (RNC)	As above but neighboring cells recruited to streak if > 60% surrounded by streak cells	Fully formed streak	8	Stern and Canning (1990), Eyal-Giladi et al. (1992), Lawson and Schoenwolf (2001a, b)
BMP + DCM + RNC + Migration of streak cells out of epiblast (MSC)	As above but cells begin to leave the streak after stage 3+	Maintenance of fully formed streak; composition of streak shifts to new recruits	9	Eyal-Giladi et al. (1992), Psychoyos and Stern (1996)
BMP + DCM + *reduced* RNC + MSC	As above, but criteria for recruitment of cells increased to 80%	Preferential loss of posterior streak	10	Canning et al. (2000)

Further details regarding the procedures used are provided in the text and Table 2; The initial pattern for all simulations (except that shown in Fig. 4) is provided in Fig. 5a.

However, most cells remain near the posterior pole and those that are incidentally distributed along the midline do not extend as far anterior as does the streak.

2.3. Elongation of the streak—oriented cell division

Wei and Mikawa (2000) have suggested that streak elongation is driven by oriented cell division. They marshal the following data in their report. The progenitor pool of cells (our sickle and sickle-associated epiblast) is 23–34 cells in anteroposterior extent. This is consistent with the estimate that the width of the Koller's sickle varies from 5% to 12% of the anteroposterior extent of the *area pellucida* (Hatada and Stern, 1994). The cells and their progeny come to occupy an anteroposterior length (the streak) of about 127 cells by stage 3 (about 12 h). This six- to seven-fold increase can be accounted for by assuming that cells undergo division with a cycle time of about 4 h and that these cells maintain an axis of division parallel to the elongating streak. Detailed examination of mitotic figures confirms this orientation, albeit with some significant variation (50% of cells are precisely oriented to the anteroposterior axis and an additional 30% of cells are within 45° of this orientation).

We have examined this hypothesis as follows. Cells known to be streak precursors are highlighted in the initial model tissue (Fig. 5a). These cells and their progeny are then directed to divide with a precise anteroposterior orientation (Fig. 6). As is all simulations, the global movement pattern (Fig. 4) is present as a background phenomenon. In our model, precise mitotic orientation of streak forming cells results in minimal additional streak elongation over that seen in the absence of this orientation (compare Fig. 6 to Fig. 5b).[2] We suggest that for this mechanism to produce sufficient elongation, the axis of division must be precisely fixed with little or no variation, i.e., daughter cells that result from division along alternative axes will not span enough distance in the anteroposterior direction to generate a sufficiently long streak in the limited time (number of divisions) required. In contrast, the data (Wei and Mikawa, 2000) suggest that there is a significant spatial distribution about the preferred orientation. A further assumption of this hypothesis is that there exists a mechanism to keep the cells in precise

(*footnote continued*)
other cells (e.g. pre-forebrain cells—see Foley, et al., 2000) prior to streak formation. Thus, the streak precursors are "going with the flow" but the flow is not sufficient, by itself, to generate the streak.

[2]Indeed, most of the streak elongation seen in this simulation is secondary to the central "updraft" of the background movements. In simulations in which the central "updraft" has been removed, very little streak elongation occurs as a consequence of oriented divisions alone (data not shown).

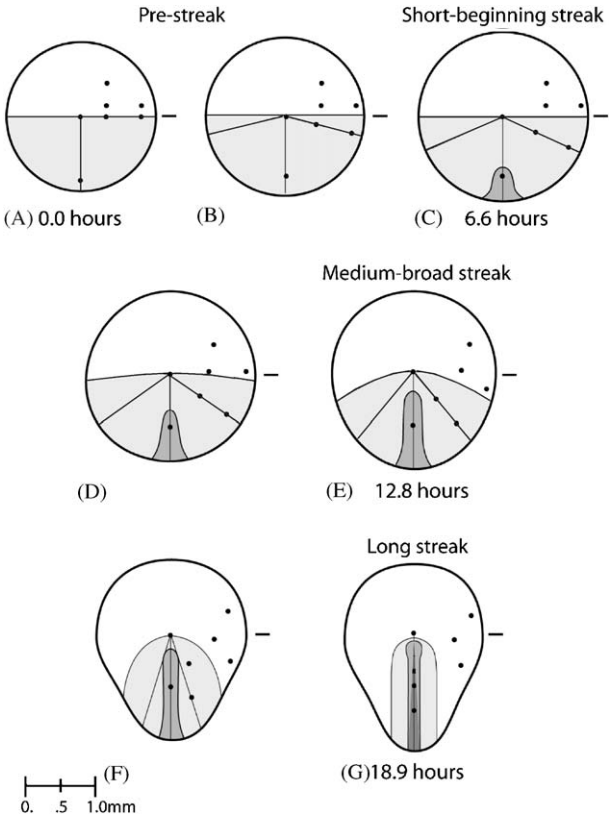

Fig. 2. Shown is a schematic summary diagram of the epiblast cell movements as defined by carbon-particle markers (after Spratt, 1946). Light stippling represents the original posterior half of the epiblast; dark stippling demarcates the emerging streak. Sequential schematics are 3 h apart and roughly correspond to (A) stage XIII, (B) stage XIV, (C) stage 2, (D) stage 3, (E) stage 3+, and (F,G) between stages 3+ and 4 (here designated, stage 3++).

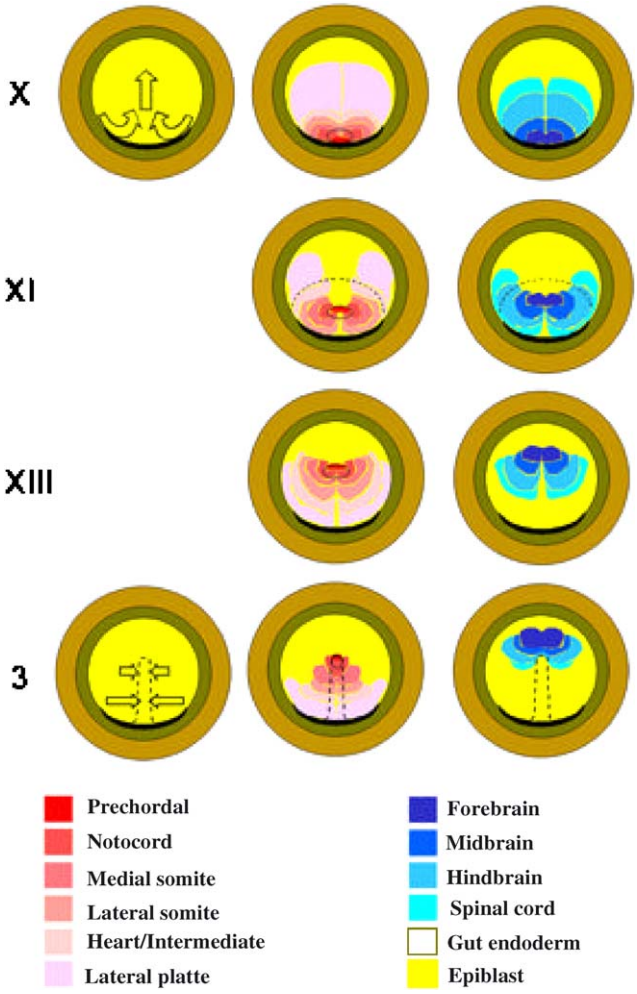

Fig. 3. Shown is a schematic of the global epiblast movement pattern and associated summary fate maps. As discussed in the text, this global movement pattern causes cohorts of cells comprising a series of dorsal-to-ventral fates to become distributed along the posterior midline (with more dorsal fates lying more anteriorly). Note that these movements begin well before streak formation; after streak formation, there is a component of direct movement into the steak from adjacent epiblast. Stages are demarcated on the left. Arrows represent the major thrust of cell movements. The dark crescent posteriorly represents Koller's sickle. The dashed line at stage XI represents the extent of the underlying hypoblast and the dashed lines at stage 3 represent the primitive streak. Reproduced from "Gastrulation: from cells to embryo" (Stern, 2004)© Claudio D. Stern (2004).

alignment. Like gymnasts stacking themselves one atop another, the alignment must be maintained or the entire column will collapse. In our model, agitation from neighboring cells causes the alignment to be disrupted (see Discussion). Although we could invoke an *ad hoc* mechanism to maintain the alignment, in the absence of data supporting such a mechanism, we suggest that oriented cell division is unlikely to be the prime mover in elongation of the primitive streak, although we cannot discount that it may contribute.

2.4. Streak elongation—streak-specific movements

The evolving streak forms by a rapid and dramatic "growth" of a cohort of cells (the sickle and sickle-associated epiblast) at the posterior pole of the epiblast (Bachvarova et al., 1998; Wei and Mikawa, 2000; Lawson and Schoenwolf, 2001a, b). Growth may occur at one end (as knitting a sock) or in an interstitial pattern (as expanding an accordion). When the initial cohort of streak-forming cells is marked experimentally in a precise anteroposterior pattern, these markings appear in register in the evolving streak. That is, the most anterior cells give rise to the most anterior streak, the most posterior cells form the most posterior streak and intermediate cells fill in the appropriate intermediate positions (Wei and Mikawa, 2000). This is consistent with an interstitial, accordion-type of growth.

We have modeled the evolving primitive streak by adding an additional movement component to cells derived from the sickle and sickle-associated epiblast. The accordion-type growth discussed above suggests a gradient in the rate of movement such that the rate

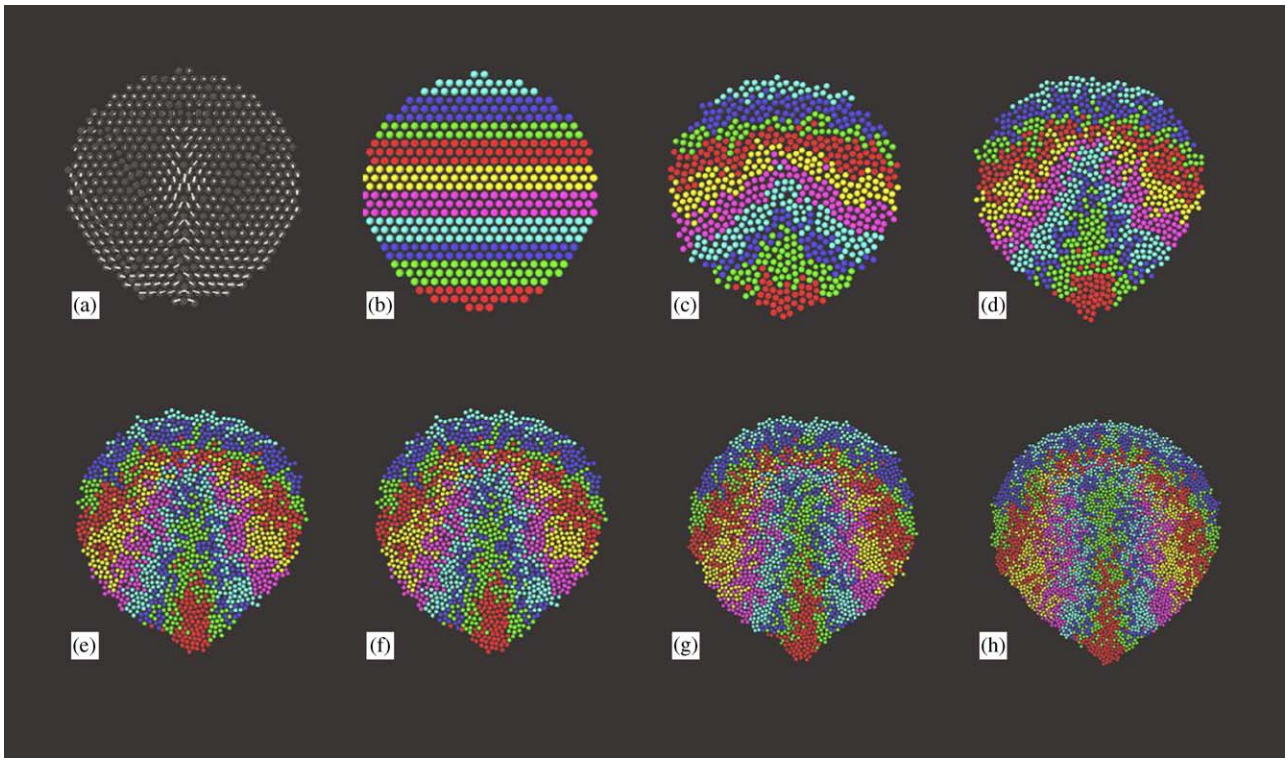

Fig. 4. Model of the chick- epiblast incorporating the global pattern of movement. To approximate the known movement pattern (see Figs. 2 and 3, Foley et al., 2000 and text), we divide the epiblast into two halves along the anteroposterior midline. Movements for each half are calculated in a similar fashion, although for the left half movements are directed counter-clockwise and for the right half they are directed clockwise. For each half, the center is determined. The movement vector direction is perpendicular to a (radial) line from the half-center to the cell center. The maximum rate of movement is set to 100 μm/h (Spratt, 1946) and internally scaled to the model epiblast (see text). We define a radial factor (R) as equal to the normalized distance (where 0.0 is at the half-center and 1.0 at the half-periphery) from the half-center to the cell center raised to a power of 1.25. The exponent of 1.25 is provided so that the periphery tends to run a little ahead of more central locations in concert with the data. An exponent value of 1.00 does not significantly alter the results (not shown). We define a circumferential factor (C) as equal to the normalized angular position where angular position is defined using the anterior pole and the "mid-epiblast" pole that is located 90° clockwise from the anterior pole on the left half (or 90° counter-clockwise from the anterior pole on the right half). Angular position is normalized to run in both directions from 0.0 at the anterior pole to 1.0 at the mid-epiblast pole. For example, on the left half, if we travel counter-clockwise 270° from the anterior pole to the mid-epiblast pole, angular position increases from 0.0 to 1.0 and if we continue on it then decreases from 1.0 to 0.0 over the remaining 90° from the mid-epiblast pole back to the anterior pole. The maximum movement per tick is then scaled by R times C. These mathematical formulations merely are meant to approximate the observed movement patterns (Foley et al., 2000 and text) and are not suggestive of any presumed *in vivo* mechanism or driving forces. In (a), line segments oriented to and proportional in length to the individual movement vectors are shown. In (b), the 502-cell initial model tissue, representing the stage XIII embryo, is shown. Cells have been arbitrarily marked (striped pattern) to allow the evolution of the gross tissue pattern to be observed. This color coding is passed to progeny and thus like colored cells form a "polyclone." The state of the tissue is shown at successive 3 h intervals roughly corresponding to stages as follows: (c) 3 h (770 cells), stage XIV, (d) 6 h (1094 cells), stage 2, (e) 9 h (1650 cells), stage 3, (f) 12 h (2393 cells), stage 3+, (g) 15 h (3526 cells), stage 3++, and (h) 18 h (5185 cells), stage 4. The images have been independently scaled so that all images are about the same size. Cell numbers per stage will vary slightly for sequential runs of the same simulation.

increases with increasing anterior position. The direction of the movement is towards a target located just anterior to the center of the tissue.[3] All cells follow the background movement pattern (Fig. 4) but the streak-forming cells add a movement component directed toward the target and with a magnitude increasing with increasing proximity to the target. This additional component is not added until 3 h of simulated development have elapsed (about stage XIV, when streak elongation is known to begin). As expected, this model produces an elongating streak (Fig. 7). However, the progeny of the streak-forming cells are strung-out along the posterior midline with a large amount of intercalation of (non-streak) cells from the surrounding epiblast. The number of streak progeny is insufficient to fill the

[3]We use the target point as a mathematical construct. Whether these cells are directed toward some positional point, or towards a defined cell population, or simply "upwards" has not been experimentally defined.

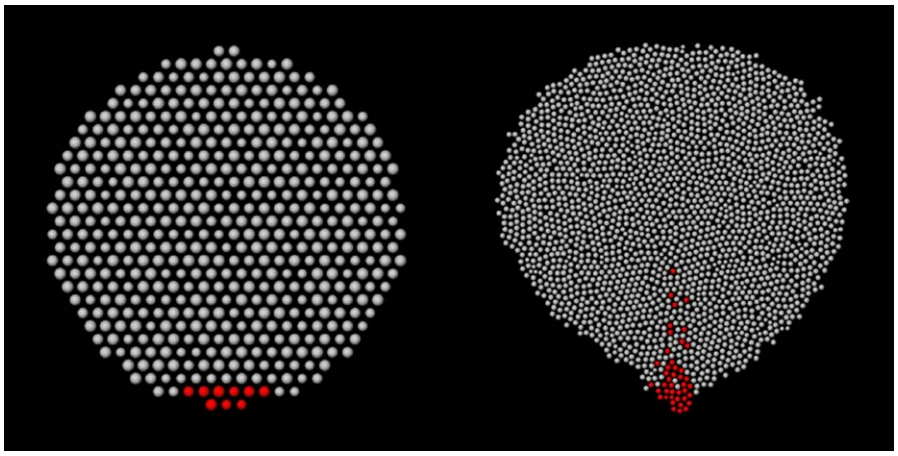

Fig. 5. The initial 502-cell pattern used for detailed simulations of the streak is shown in (a). A small cohort of cells in the posterior epiblast has been highlighted (red) to represent the sickle and sickle-associated epiblast (see text). In (b), the simulation has been run to the 12 h time point (about stage 3+) using the global movement pattern (as in Fig. 4).

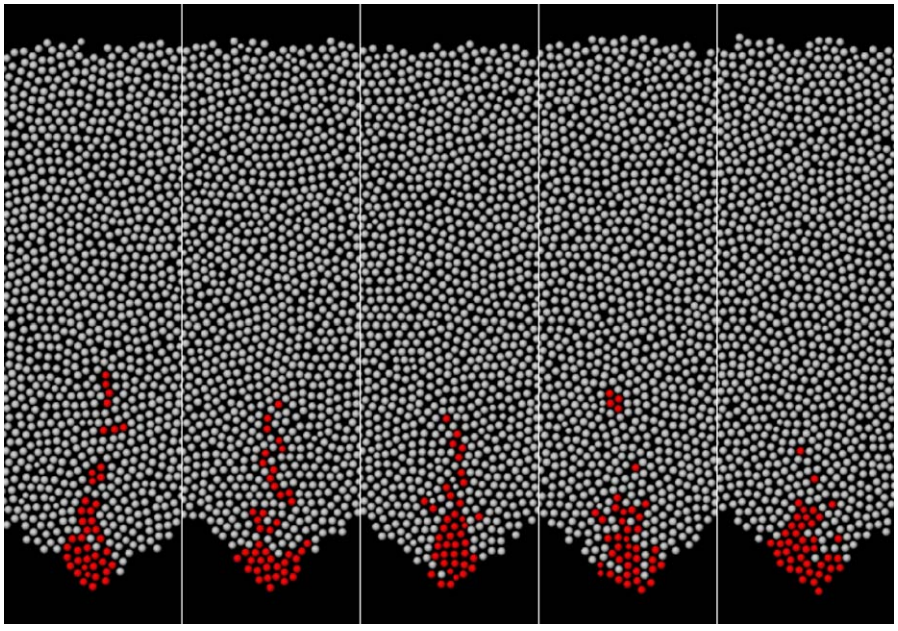

Fig. 6. In addition to the global movement pattern (see Fig. 4 and text), cells derived from the sickle and sickle-associated epiblast (red) divide with an orientation parallel to the anteroposterior axis of the embryo (Wei and Mikawa, 2000 and text). "Blow-ups" of the streak region are shown at the 12 h time point (about stage 3+). Five runs of the simulation are provided to demonstrate the degree of variability in the simulated streak.

area of the streak in its entirety and epiblast cells that enter from more lateral positions readily fill this potential void.

2.5. Filling-out of the streak

Koller's sickle and the sickle-associated epiblast are specific contributors to the streak. Other epiblast cells also appear to contribute to the streak (Stern and Canning, 1990), although the origin of these cells may be limited to those in relatively close proximity to the midline (Eyal-Giladi et al., 1992; Lawson and Schoenwolf, 2001a, b). We have therefore added a mechanism for conversion of non-streak epiblast cells to primitive streak cells.[4] In this simulation, cells largely surrounded by streak cells (>60%) convert to streak cells—a "community effect" (Gurdon, 1988); these newly

[4]An alternative, that cell proliferation in the streak is much greater than that of the surrounding epiblast and thus allows the streak to fill itself out seems excluded by the available data (Stern, 1979; Sanders et al., 1993).

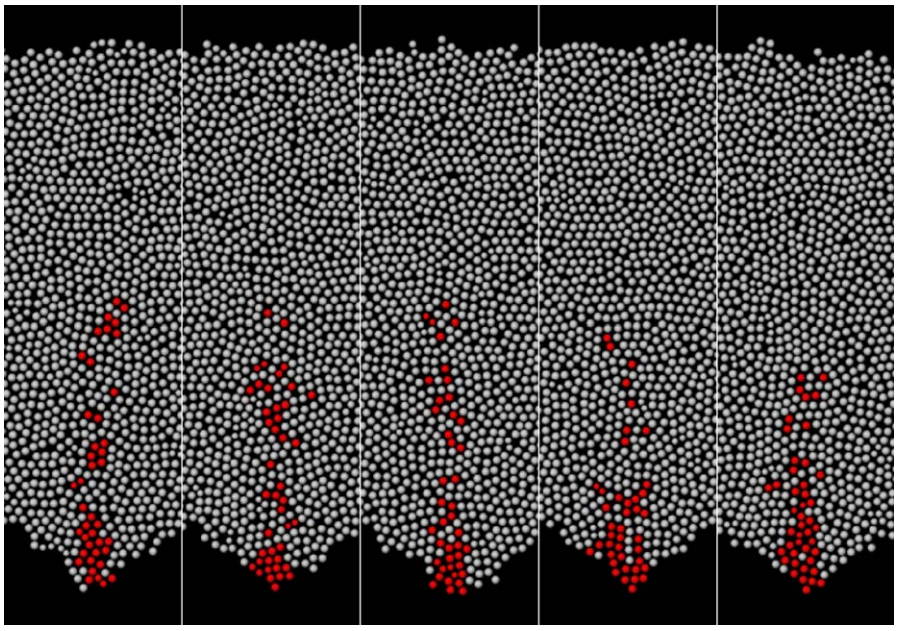

Fig. 7. In addition to the global movement pattern (see Fig. 4 and text), cells derived from the sickle and sickle-associated epiblast (red) actively move toward a target located just anterior to the center of the epiblast (see text). This added movement components begins at the 3 h time-point (about stage XIV). To model this movement component, we define a radial factor (R) as equal to the normalized distance (where 0.0 is at the target and 1.0 at the epiblast periphery) from the target to the cell center, and the maximal rate of movement (MM) as equal to 165 μm/h. Then the magnitude of the additional streak movement component is $(1.0 - R) \times MM$. The rate of cell movement toward the target accelerates as cells approach the target. This mathematical formulation merely is meant to provide a method for concretizing a movement pattern consistent with the cell marking data (see text); no specific *in vivo* mechanism or driving force is implied. However, a feature of this construct is that cells migrate toward a target. Whether such a pre-designated target exists and whether, for example, some defined cell cohort constitutes such a target is unknown. "Blow-ups" of the streak region are shown at the 12 h time point (about stage 3+). Five runs of the simulation are provided to demonstrate the degree of variability in the simulated streak.

recruited streak cells then act in every way (e.g. movement pattern, conversion of other cells) like cells derived from the original streak forming cells. This produces a fuller streak (Fig. 8), as seen in the embryo.

2.6. Steady-state streak

Throughout the period of growth of the primitive streak, cells continue to enter the streak from the epiblast and, after stage 3+, begin to exit the streak to deeper levels (Psychoyos and Stern, 1996). We do not know the mechanisms that control this influx and efflux of cells into and out of the streak. The rapid enlargement of the streak cannot be explained on the basis of mitoses alone (see above; Stern, 1979; Sanders et al., 1993) and, therefore, must include a significant rate of cellular entry and recruitment from within the epiblast. In addition, maintenance of the streak after stage 3+ requires that growth within, and additions to, the streak must at least keep pace with cellular egress to deeper layers.

Within our two-dimensional model cells cannot exit the plane of the epiblast. Therefore, we mimic the phenomenon of cellular egression to deeper layers by having cells within the plane gradually shrink and disappear—a geometrically equivalent action from the perspective of the epiblast plane (see Appendix B). Neither the controlling parameters nor the exact spatial distribution of this cellular egress is known. Therefore, we only can model this phenomenon in the broadest sense and with a fairly arbitrary scheme for which cells leave the streak and when. In our simulation, cells must be resident in the streak for some set period of time after which they leave the streak with a probability that increases with increasing residence time (Fig. 9). One result is that cells derived from the sickle and sickle-associated epiblast cells disappear preferentially relative to recruits from the surrounding epiblast (compare Fig. 9 to Fig. 8). This has been described *in vivo* (Eyal-Giladi et al., 1992).

In our model, the *posterior* streak is maintained by a balance of: (i) cell addition from the epiblast versus (ii) cell loss by anterior migration and egress (after stage 3+) into the deeper layers. The *anterior* streak is maintained by a balance of: (i) cell addition from the epiblast and anterior migration of more posterior cells versus (ii) egress (after stage 3+) into the deeper layers. Thus, migration within the streak supports the anterior

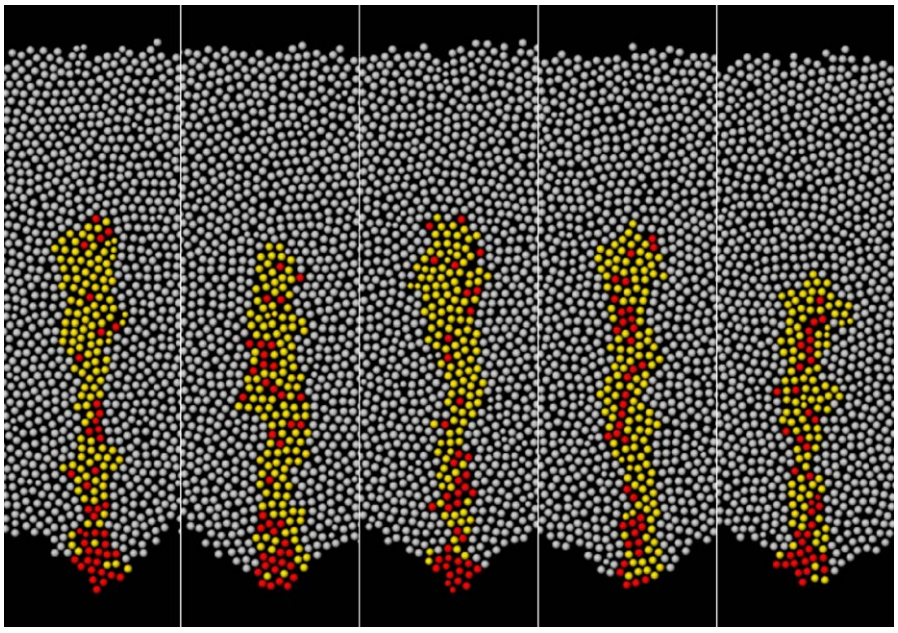

Fig. 8. In addition to the global movement pattern and the streak-specific movements (Fig. 7), non-streak epiblast cells convert to streak cells if more than 60% of their near neighbors are streak cells. Original cells, derived from the sickle and sickle-associated epiblast (red), are distinguished from recruits (yellow). "Blow-ups" of the streak region are shown at the 12 h time point (about stage 3+). Five runs of the simulation are provided to demonstrate the degree of variability in the simulated streak.

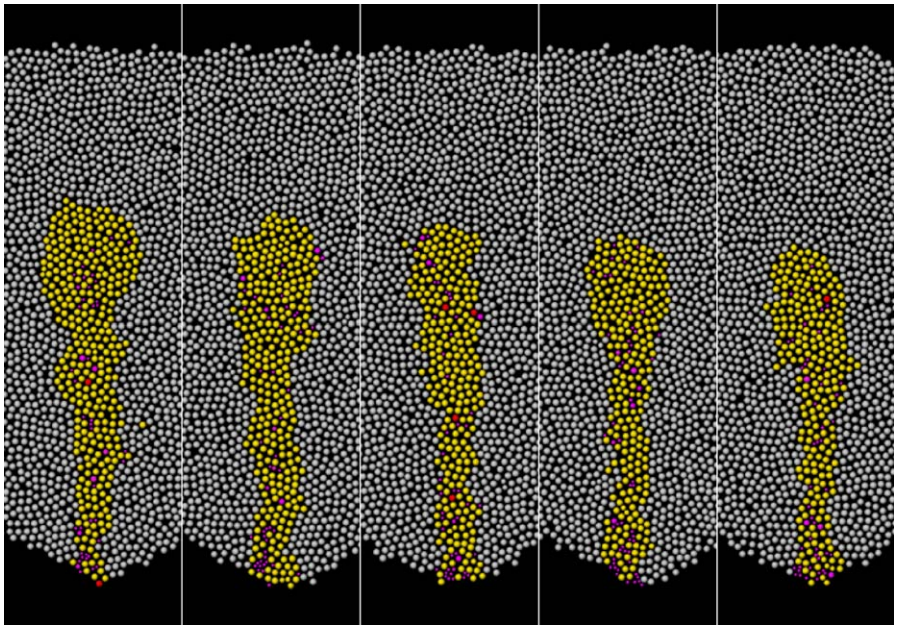

Fig. 9. In addition to the global movement pattern, the streak-specific movements and incorporation of non-streak cells into the streak (Fig. 8), streak cells begin to exit the streak by migrating into the deeper levels (modeled here using a cell death algorithm as discussed in Appendix B). Cells must maintain residence in the streak for at least 12 h, after which they leave with a probability that increases with increasing time of residence (defined by an erf function with S.D. = 3 h). Cells "caught in the act" of leaving the streak are identified (purple). "Blow-ups" of the streak region are shown at the 15 h time-point (about stage 3++). Five runs of the simulation are provided to demonstrate the degree of variability in the simulated streak.

streak at cost to the posterior streak, and the posterior streak is more sensitive to cell loss. Along these lines, the posterior streak should also be more sensitive to a decrease in recruitment of epiblast cells. Simulations run in which the criterion for recruitment is more restrictive (and fewer cells are therefore added) do, indeed,

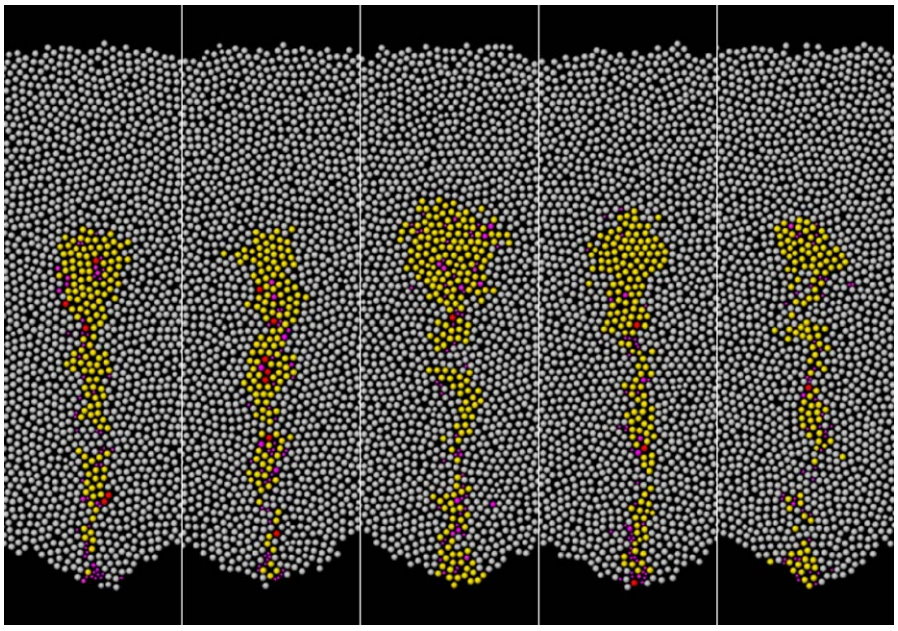

Fig. 10. The simulations presented in Fig. 9 are repeated. However, to mimic an experimentally induced hindrance to epiblast cell recruitment into the streak (Canning et al., 2000), the criterion for recruitment of cells into the streak becomes more stringent (>80% versus >60%—as defined in text and Fig. 8) after the 9 h time point (about stage 3). "Blow-ups" of the streak region are shown at the 15 h time point (about stage 3++). Five runs of the simulation are provided to demonstrate the degree of variability in the simulated streak.

demonstrate a disproportionate disruption of the more posterior streak (Fig. 10). In fact, interference with movement of new epiblast cells into the streak *in vivo* (Canning et al., 2000) causes preferential loss of the posterior streak that is consistent with this type of "steady-state" mechanics.

3. Discussion

Formation of the primitive streak remains a dramatic but poorly understood milestone in amniote embryogenesis. In the chick, the streak forms rapidly between stage XIV and 3+, a time window of less than 12 h. The streak appears to arise from a precursor population of cells in the extreme posterior epiblast that rapidly deploys along a radius, to define the anteroposterior axis.

In analysis of their elegant cell marking study of primitive streak formation, Wei and Mikawa (2000) suggest that sequential, oriented cell division could account for streak elongation. This theory fails in our simulations because: (i) without an additional *ad hoc* mechanism to maintain cell alignment the necessary cell "stacking" falls victim to the exigencies of local cell–cell jostling and small realignments (see below), and (ii) the number of cells produced may be able to span the length of the streak but will not be able fill it out sufficiently.

Our simulation results suggest that the primitive streak is the product of a pattern of directed cell migration coupled with recruitment of neighboring epiblast cells. These mechanisms can account for rapid elongation, filling out and maintenance in the face of cell loss into the deep layers. In addition, two experimental findings, a shift in the cellular composition of the streak from precursor progeny to new recruits (Eyal-Giladi et al., 1992) and the preferential loss of the posterior streak when recruitment is inhibited (Canning et al., 2000) are explained.

Our simulations cast the streak as a emerging from a dynamic program that includes movement and division of a defined cell population, recruitment of neighboring cells to this population and a time-dependent loss of cells from the population.

We recognize that verisimilitude in our simulated embryo depends on the ability of our computer simulations to capture the salient features of the *in vivo* system and to avoid artifacts which might be destructive to this end. We, therefore, address these issues in some detail below:

3.1. Cell mixing

All simulations demonstrate a limited degree of cell mixing. That is, near-neighbor relations become locally disturbed but neighboring cells and their progeny do not become widely separated. It has been previously shown that cell mixing is a consequence of interstitial cell division (Bodenstein, 1986). Given the interstitial mitotic pattern known to be present in the epiblast

(Derrick, 1937; Stern, 1979; Sanders et al., 1993) some degree of mixing is to be expected. Active cell movement enhances this dispersion even if cells are programmed to move as a cohort. Although experiments directly designed to quantify cell mixing in the epiblast are lacking, there is evidence that some such mixing does occur. First, cine analysis appears to show some jostling of individual cells relative to their neighbors superimposed on the more coordinated (cohort) movements (Foley et al., 2000). Second, when small groups of contiguous cells are marked and then followed for several hours, the resulting pattern shows some degree of local dispersion (Wei and Mikawa, 2000). Third, fate map analysis has shown that contiguous groups of cells do not necessarily maintain proximity to other groups of cells (Hatada and Stern, 1994), as has been found for other species whose topology during gastrulation is a flat disc or blastoderm (Ho, 1992; Helde et al., 1994; Wilson et al., 1995).

We expected our model tissues to show more cell mixing than in the actual embryo because our model cells are inelastic and much fewer in number. Cell mixing secondary to interstitial mitotic activity is generally confined in magnitude to a few cell diameters. The mixing is directly counterpoised by the "anti-mixing," (i.e. growth) of cell patches by mitosis. A large patch of cells will not be disrupted but will develop variable degrees of "raggedness" at the edges. A small patch, however, will demonstrate much more disruption (Fig. 11). At the cell level the degree of mixing is the same, but the gross appearance is quite different. This is because proportionally more of the small patch is composed of edge—the perimeter to area ratio (2D) or surface area to volume ratio (3D) is greater. Our model tissue has many fewer cells than the corresponding real tissue (e.g. our initial tissue of about 500 cells is designed to model the stage XIII epiblast of perhaps 20,000–50,000 cells). In our model, the sickle and sickle-associated epiblast and their progeny forms an even smaller cohort and we can expect more apparent disruption in the model than *in vivo*.

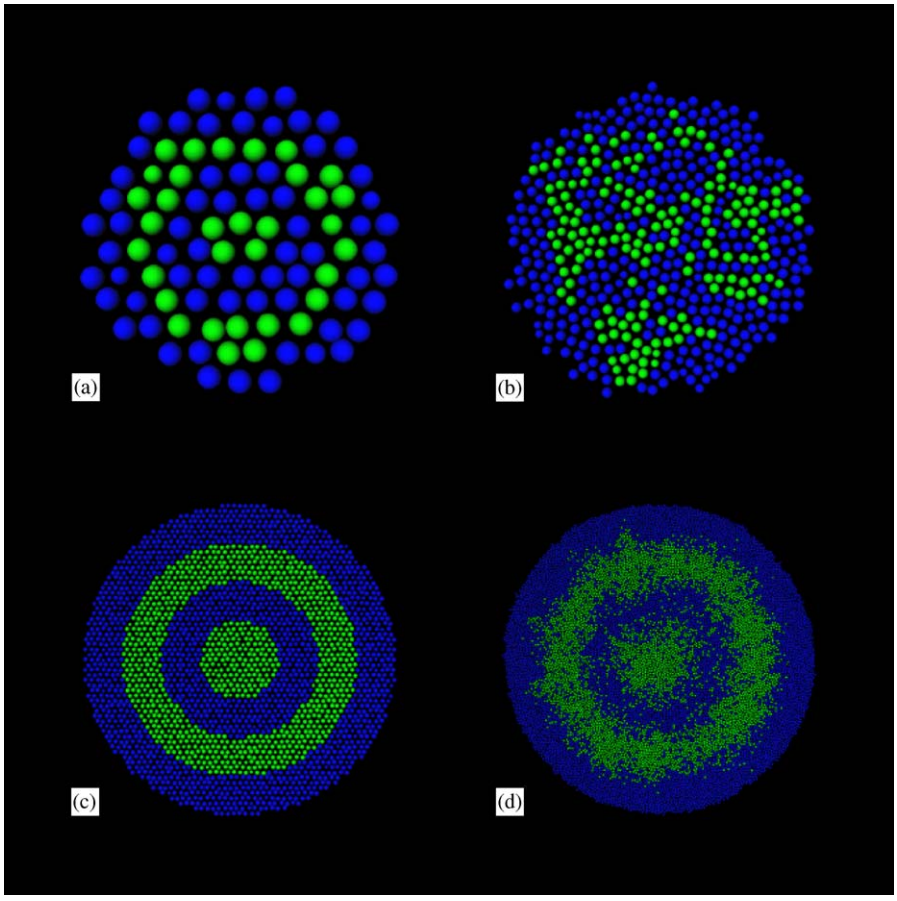

Fig. 11. Demonstration of the effect of patch size on apparent cell mixing. Starting patterns are marked in concentric rings of width equal to about 25% of the radius of the disk. Simulations are run until the cell number has increased five fold. In the first case, the initial "tissue" has about 100 cells (a) and is run to about 500 cells (c). In the second case, the initial pattern has about 2500 cells (b) and is run to about 12 500 cells (d). Note that concentric rings are readily apparent in the larger tissue (d) but not evident in the small tissue (c) despite similar simulation parameters (see text).

3.2. Simple representation

We have produced a highly simplified, cartoon version of the primitive streak embryo. We have only examined the epiblast and this has been represented as a planar sheet of cells. Finally, we have modeled the individual cells as simple, inelastic spheres. Our simulations pointedly lack a "real physics" of cell–cell interactions (see Keller, 2002). Cells are manipulated on a geometrical basis and no true forces are modeled. Indeed, there are, as yet, no available data on the forces which act upon individual cells in the epiblast.

Although the epiblast is not precisely planar, it is very nearly so. This simplification reduces computation time and avoids us having to postulate the means by which the cells are maintained in a sheet (i.e. in a curved sheet in three-dimensional space, some mechanism must be invoked to keep the cells in line, whereas if the simulation is confined to a plane, we merely enforce the inherent condition that the z-coordinate is zero). The use of spheres to represent cells dramatically reduces computation time and is justified since we are examining gross tissue patterns and not details involving a single cell or tiny groups of cells. In fact, there are virtually no data on the geometry of individual cells or the physics of their interactions during morphogenesis of the epiblast. The most significant confounding artifact from our simplification as it affects gross tissue patterns is the propagation of local events to distant points in the tissue. We have, therefore, specifically sought to address and minimize this artifact (see Appendix B—Nudge Event).

Unlike the remainder of the epiblast, the primitive streak is multi-cellular in depth (rev. Romanoff, 1960; rev. Patten 1971). We have confined our current simulations to a single-cell layer and make no attempt here to simulate this depth.

Further inquires will require that we fill-in our simple cartoons and add full three-dimensionality and, eventually, a real physics of interactions (e.g. forces). Certainly, it will be necessary to add additional cell layers (e.g. hypoblast) and important cell populations (e.g. marginal zone). In particular, we are keenly interested in the effect of the hypoblast on the global cell movement pattern in the overlying epiblast and in positioning of the streak (Waddington, 1932; Foley et al., 2000).

3.3. Variability

Successive runs of any given simulation will produce patterns that vary slightly in detail but readily are recognized as thematically consistent—variations-on-a-theme. For this reason, several runs of most simulations are presented. In the model, some variables have been precisely defined (e.g. the vector of active cell movement, division volume) others have a stochastic component (e.g. cell-cycle time, orientation of cell division). Where the number of cells is large, the variation appears proportionally more muted; whereas, where a small number of cells is involved the variability seems proportionally greater. Because our model tissue consists of a small fraction of the number of cells in the real tissue, we tend to see more variability than might be present in nature. Although requiring some caution when examining results, we view this variability as a distinct plus for the model; it is more consistent with nature than would be a precise, "cookie-cutter" patterning generating machine. At a more philosophical level, the ability to generate a fixed global pattern by pooling of elements whose structures and behaviors are themselves stochastic is a defining feature of the morphogenesis of complex organisms.

Appendix A. The early chick embryo (a primer)

We have chosen to study the early chick embryo and the initiation, extension and maintenance of the primitive streak. We focus on stage XIII through stage 3 (Hamburger and Hamilton, 1951; Eyal-Giladi and Kochav, 1976), although some simulations have been extended to around stage 4. Under normal conditions these events take place over a period of about 12–18 h (Romanoff, 1960; Patten, 1971; Stern, 2004).

A.1. Gross morphology

At stage XIII, the embryo consists of a roughly circular disc, the *area pellucida*, surrounded by a halo, the *area opaca* (Fig. 1). A *marginal zone* defines the boundary of the *area pellucida*. The dorsal surface (away from yolk) of the *area pellucida* is the *epiblast;* the ventral surface consists of populations of cells that form the emerging *hypoblast*. The hypoblast is most complete in the posterior region but gradually enlarges and coalesces to subtend most of the epiblast. Between the epiblast and hypoblast a *mesoblast* eventually forms to establish the tri-laminar embryo. On the anterior surface of the posterior aspect of the marginal zone there is a morphologically distinct crescent of cells (*Koller's sickle*).

Beginning at about stage XIV, the primitive streak forms in the region of Koller's sickle and gradually extends in an anterior direction. This streak will eventually regress but serves to define the future anteroposterior axis of the embryo. At the most anterior aspect of the streak is the amniote equivalent of Spemann's organizer, *Hensen's node.* As the streak is established it develops a groove along its length through which epiblast cells appear to migrate into the subjacent layer.

The cells of Koller's sickle lie in a plane just beneath the epiblast. It is the epiblast cells which overlie Koller's sickle (here termed, *sickle-associated epiblast*), along with cells from Koller's sickle proper, that contribute to the primitive streak (Stern, 1990; Eyal-Giladi et al., 1992; Bachvarova et al., 1998; Wei and Mikawa, 2000; Lawson and Schoenwolf, 2001b).

Beginning at about stage 3, the shape of the embryo changes by an extension in the anteroposterior direction and results in an elongated embryo with a diminished width in the posterior region relative to the anterior region ("upside down pear-shape"). This caudal elongation, both of the embryo as a whole and of the primitive streak, begins after establishment of the streak and becomes increasingly more pronounced at later stages.

A.2. Cell movements

A dramatic, global pattern of cell movements characterizes the epiblast before and during the stages under study (Gräper, 1929; Wetzel, 1929; Spratt, 1946; Eyal-Giladi et al., 1992; Hatada and Stern, 1994; Foley et al., 2000; Lawson and Schoenwolf, 2001b; Romanoff, 1960). Spratt (1946) used a carbon-particle marking system to describe these cell movements from the "pre-streak" to the "long streak" stages. Cells move circumferentially from anterior to posterior. The rate of movement increases with increasing angular distance from the anterior midline and with increasing radial distance from the tissue center (Fig. 2). Cells appear to move *en masse* but not as a fixed sheet, and independence of movement amongst the cells has been noted (Hatada and Stern, 1994). As a consequence of these movements, the area extent of the original anterior half of the epiblast increases and the area extend of the original posterior half decreases. According to Spratt, much of the former is accomplished by increasing cell numbers secondary to cell division and much of the latter by ingression of the posterior epiblast into the primitive streak. In the earliest (pre-streak) stages, the epiblast increases in size to accommodate the increasing cell number and during the latter stages (after emergence of the streak) there is a dramatic posterior elongation of the tissue silhouette. Beyond the general circumferential movement there is an active "updraft" (toward anterior) in the posterior midline during the pre-streak and evolving streak stages (Eyal-Giladi et al., 1992; Hatada and Stern, 1994). In addition, cells migrating upward in the midline appear to burst forth just beyond the mid-embryo in a pattern reminiscent of a fountain (Foley et al., 2000). The overall pattern of movement has been described as "polonaise" (Gräper, 1929) or more fully as a "double-whorl" (Wetzel, 1929).

Another view of these movements is provided by serial fate map analysis (Fig. 3; Hatada and Stern, 1994). As early as stage X, cells at the posterior margin of the epiblast begin to circumferentially converge toward the posterior pole and then move anteriorly along the posterior midline. Thus, a bilateral sequence of dorsal-to-ventral cells fates is "folded" in register into the posterior midline such that cells having more dorsal fates come to lie in more anterior locations. One consequence of this global pattern is that a population of cells destined to contribute to the forebrain is displaced (or moves) along the posterior midline from a location at the posterior pole to a far more anterior position (Foley et al., 2000). Later, the primitive streak elongates along a similar path and reaches just shy of the final location of these forebrain precursor cells. In addition, once the primitive streak is evident, there appears to be a direct movement of cells into the streak from the adjacent epiblast.

A.3. Mitotic activity

There is a regional variation in mitotic activity with higher activity at the edges of the epiblast and along the primitive streak (Derrick, 1937; Stern, 1979). When mitotic activity in the stage 5 embryo is corrected for cell density, cell generation time ranges from 2 to 10 h and lessens as one moves from rostral to caudal in both the epiblast and primitive streak (Sanders et al., 1993).

Within the region of the evolving primitive streak, cells division appears to be generally but not exclusively oriented inline with the long axis of the streak; this is in contrast to the remainder of the epiblast in which no such orientation is noted (Wei and Mikawa, 2000).

A.4. Cell death

Programmed cell death does not appear to be significant in the pre-streak epiblast (Bellairs, 1961). Later stages are characterized by a limited, homogeneous pattern with some increase in the anteroposterior epiblast (Bellairs, 1961; Sanders et al., 1997) and an additional, discrete component in the midline (Kelly et al., 2002).

Appendix B. The model

B.1. Overview

Nudge++ is a general and generalizable system for modeling morphogenesis.[5] Its conceived structure is designed to allow the model to be readily tailored to any given system. In the model, tissues are constructed as cohorts of individual, geometrically distinct, cells. Morphogenesis of the tissue is shaped by the summed

[5]*Nudge*++ is a product of Olana Technologies Inc.

behavior of these cells. In turn, this behavior is driven by internal cellular programs of arbitrary complexity.

B.2. Design

The model and its program implementation use object-oriented design in contrast with an earlier prototype (Bodenstein, 1986). All major components of the model are modular and can be added, removed or modified on an individual and independent basis. The set of modules is expandable to allow the introduction of novel components.

The fundamental class is the *cell*. A cohort of cells forms a *tissue* or *organism*. Cells possess *states* and exhibit *actions*. Each state or action is likewise structured as a class. For example, each cell possesses a three-dimensional form defined by a *shape* class. Shape may be coded as a constructive geometric form (e.g. sphere, ellipsoid) or a polyhedron (or by means of an alternatively defined scheme). By selecting or providing the appropriate module (class definition) one can readily incorporate and change the nature of the representation without restructuring the entire program. In addition to physical entities (e.g. shape), interactions and events (e.g. cell–cell adhesion, mitosis) are also formulated as classes.

B.3. Implementation

The core program is written in C++ (Stroustrup, 1997) under Linux. The interface combines Motif, Mesa (an OpenGL® API surrogate) and Open Inventor™.[6] All supporting software packages are standard issue and thus the model "ports well" between platforms.

B.4. Time

A *tick* is the smallest unit of simulation time. In practice, a tick is set to represent some unit of real-world time appropriate for the system under study (e.g. 5 min for our chick embryo). All events within a single tick are presumed to occur simultaneously, i.e. within the tick "time bin." In practice, the many thousands of program events occurring within a single tick actually take place sequentially within the program.

During each tick, each cell is evaluated based on its states and its environment. Actions are generated and these actions may or may not affect other (usually neighboring) cells.

[6]OpenGL® and Open Inventor™ are trademarks and/or registered trademarks of Silicon Graphics Inc. in the United States and other countries. Mesa is an Open Source product based on the published OpenGL® API, but is not an implementation which is certified or licensed by Silicon Graphics Inc. under the OpenGL® API.

B.5. Space and geometry

In the model, a *click* is defined as a uniform unit of spatial dimension; one click can be assigned to any real-world measurement (e.g. one micron for our chick embryo). Clicks, however, are not minimal spatial units and fractions of clicks are valid.

The model functions in two- or three-dimensional space. In the "two-dimensional" case, cells themselves are three-dimensional but they are confined to a plane. Cells are not confined to a fixed spatial array but may have any coordinate position in two- or three-dimensional space, respectively.

B.6. Cell states

The baseline list of cell states includes *age* (time since last mitosis) *phase*, *phase-age* (time since last phase change), *generation*, *clone* and *lineage*. As noted above, states are defined as classes and additional states may be selected or added on an *ad hoc* basis. For example, a *general cell state* class allows an unlimited number of arbitrarily specified numerical states (e.g. the concentration of some compound, whether or not a specific gene is active, etc.). Another *cell tag* class allows cells to be tagged at arbitrary times with "vital stains" in order to visually trace lineage and make comparison with experimental marking experiments.

B.7. Environment

Cellular environment refers to surrounding cells, local extra-cellular features (e.g. a boundary) and general position within the organism. This may involve near-neighbors (abutting cells), local neighbors (cells within some range), "local" positional factors (e.g. on an edge) and "global" position (e.g. in the anterior one-fourth of the organism). Positional information (Wolpert, 1969, 1971) may be defined as an environmental variable or as a cell state or combination of states (e.g. Gierer and Meinhardt, 1972).

B.8. Actions

Major actions are those that affect cell geometry (shape and position). These include *growth*, *division*, *movement* and *death*. A key component of geometric actions is the *nudge event*. In a close-packed or somewhat close-packed array of cells, any change in cell geometry will require geometric adjustment of the neighboring cells. In turn, the neighbor's neighbors may be affected, and so forth. The nudge event (see below) encapsulates these propagated actions. Changes of cellular state are minor actions and do not generate geometric alterations.

B.9. Details of the model as applied to the chick embryo

We have modeled the epiblast as a disk of cells confined to a plane. Cells are modeled as simple, inelastic spheres of volume 525 μm^3 (equivalent to a radius of about 5 μm). As spheres, cells have no geometrical orientation except during division. Our initial tissue is designed to represent a stage XIII epiblast. The actual epiblast at this stage has a diameter of about 1.1 mm and may contain about 20 000–50 000 cells. Our model "mini-epiblast" disk with its 502 cells has a diameter of about 0.28 mm.

Distance in the model is defined in terms of clicks. Here a click is set to 1.0 μm. In order to match our simulated mini-epiblast with the larger, real-world embryo the model scales relevant input data. For example, if we specify that a cell is known to move 100 μm/h in the real-world epiblast, the model will internally scale this input datum so that a model cell will move the same proportional distance in our mini-epiblast.

The tissue is formed from the collection of cells. The initial shape is that of a disk but this evolves over time. The change in tissue shape results from the pooled behavior of individual cells. In these simulations, there are no defined boundary conditions and "edge" cells behave in a similar fashion to other cells.

The model proceeds through iterations (ticks). Each tick is assigned a real-world value of 5 min; biologically relevant times can be specified in real time and converted internally to iterations. For example, if we specify the M-phase of a cell as 30 min in length, the model will maintain the cell in M-phase through six ticks.

During one *tissue tick* (one iteration for the complete tissue), each cell undergoes a *cell tick* (one iteration for the individual cell). Cells are accessed at random (using a standard pseudo-random number generator) from a diminishing pool of cells that have yet to be accessed, until all cells in the tissue have been accessed.[7]

When a cell is accessed, (i) an *evaluation* is performed based on cell states and environmental factors, (ii) action parameters are generated from the evaluation, and (iii) any specified *actions* are then performed. For example, the evaluation may determine whether or not a cell is to divide and, if so, what the orientation will be. The action would then be division of the cell in accord with this orientation. The combination of evaluation and action completes a cell tick.[8]

The nature of the evaluations and actions for the simulations in this study, tabulated in Table 2, are described in detail as follows:

- *CYCLE CHANGES*: Cell cycle is divided into standard phases (G1-phase, S-phase, etc.). Cells in the initial tissue (500 cell stage) are assigned to cell cycle positions on a random basis (e.g. 5 min into G1-phase, 15 min into S-phase). The cycle evaluation determines the length of each phase. Since in the current simulations individual phases are not used (except where M-phase precipitates division), the distinction between G1-, S-, and G2- and M-phases is largely transparent to the program and the net result is simply a total cell cycle of some defined length. Experimental data regarding the length of individual cell cycle phases in the early chick embryo is limited and for the simulations the following strategy has been used: Cycle length is known to range from two to 10 h (Sanders et al., 1993). We set M-phase to 28 ± 7.3 min (after Stern, 1979). We then make S- and G2-phase arbitrarily short to allow total cycle time to be varied by adjusting the length of G1-phase (since S + G2 + M will always be less than the desired total cycle time). The model then calculates total cycle time and G1-phase length to produce a doubling of the cell population in somewhat less than 6 h (Stern, 1979; Sanders et al., 1993). For this calculation, we assume that the mitotic index is uniform throughout the tissue.[9] Cells move from, say, G1-phase to S-phase when they have resided in G1-phase for a period of time (number of ticks) equal to the projected length of G1-phase. The transition to M additionally requires that the requisite volume of 525 μm^3 be reached, but because of the growth dynamics (see below) this criterion is always met by the end of G2-phase. The end of M-phase initiates cell division and, in turn, exiting from M-phase requires cell division.
- *GROWTH*: Cells are programmed to grow by fixed volume increments during G1-phase until the maximal size (525 μm^3) is reached. The increment is set at 100 μm/tick and daughter cells reach full size in a few ticks after division. Changing the size of the increment produces comparable results (data not shown).
- *DIVISION*: Cells divide when they reach the end of M-phase. Cell division is symmetric for volume with each daughter at half the volume of the parent cell. Daughters begin life at the start of G1-phase. Unless otherwise noted, cell division proceeds with random

[7]Each cell is accessed once-and-only-once during each tissue tick (synchronous access). The alternative strategy, whereby the once-and-only-once rule is not used (asynchronous access), produces comparable results (not shown).

[8]For each cell, actions are performed immediately after the evaluation. The alternative strategy, whereby all cells are evaluated first and then all cells perform actions afterwards, produces comparable results (not shown).

[9]Results with and without addition of the known spatial variability in mitotic index (Derrick, 1937; Stern, 1979; Sanders, et al., 1993) are similar (not shown). We have therefore used the simpler, homogeneous pattern to avoid adding another confounding variable.

Table 2
Shown is a summary table of the cell tick algorithms used in all of the simulations in this study

Category	Condition	Result	Figures						
			4	5b	6	7	8	9	10
EVALUATIONS									
CYCLE	Always	Calculate phase lengths	X	X	X	X	X	X	X
STATES	ns cell AND >60% of neighbors are s cells	Convert to s cell					X	X	
	Above, but change 60% to 80% after stage 3	Convert to s cell							X
GROWTH	Cell volume $<525\,\mu m^{\wedge 3}$ and phase = G1	Set growth flag; set growth amount to min($100\,\mu m^{\wedge 3}$, $525\,\mu m^{\wedge 3}$—current volume)	X	X	X	X	X	X	X
MOVEMENT	Phase ≠ M	Set movement flag; determine cell's position within tissue and calculate movement vector from cell position	X	X	X	X	X	X	X
	Phase ≠ M and s cell and $t>3$ h	Add "streak-specific" movement component				X	X	X	X
DIVISION	Beginning of M	Pick random division orientation vector	X	X		X	X	X	X
	Beginning of M and ns cell	Pick random division orientation vector			X				
	Beginning of M and s cell	Make orientation vector parallel to AP axis of epiblast			X				
	End of M	Set division flag	X	X	X	X	X	X	X
DEATH	Never	(death flag not set)	X	X	X	X	X		
	Phase ≠ M and s cell and if sufficient time in streak	Set death flag						X	X

Category	Action
ACTIONS	
DEATH	If flag set, eliminate cell by gradual shrinkage until gone
GROWTH	If flag set, increment volume by specified amount
MOVEMENT	If flag set, move cell by specified vector
DIVISION	If flag set, divide cell in accordance with orientation vector
CYCLE	Increment phase-age (time spent in current phase); if phase completed, convert to next phase

The procedures are processed from the top down, first the evaluation procedures, in sequence, and then the actions, in sequence. The evaluation procedures that are used for each specific simulation are identified by the x's on the right side of the table corresponding to the figure in which the simulation is presented. As described in the text, the cell death action in the model is used as a surrogate for cells migrating out of the plane of the epiblast *in vivo*. s cell—streak cell, ns cell—non-streak cell.

orientation within the plane of the epiblast. In one case (see Section 2.3 and Fig. 6), we assigned a subset of epiblast cells as "streak forming" and, in this particular simulation, cells of this subset divide with an orientation precisely parallel to the anteroposterior axis of the epiblast.

- *MOVEMENT*: Cells exhibit an active, enforced movement based on position within the model epiblast. Active movement does not occur during M-phase. Movement consists of simple displacement from a point a to point b. The position-dependent vectors which define this movement are established by the data (Fig. 2 and Foley et al., 2000) and are taken as a given baseline for the current simulations (Fig. 4). In addition, in some simulations a separate movement component has been added to "streak" cells (see Section 2.4 and Fig. 7). This latter component is suggested by the available data and is part of the set of hypotheses examined in the model.
- *DEATH*: There is no true cell death in these simulations. Cell death is used in where necessary (see Section 2.6 in main text and Figs. 9 and 10) to mimic cells leaving the plane of the epiblast. Since these simulations are done with *Nudge*++ in two-dimensional mode, cells cannot actually move off of the plane. As part of the "death program" these cells

slowly shrink in size until they are gone; from the point-of-view of the planar epiblast the effect of cells shrinking away versus leaving the plane are equivalent

- *STATE CHANGES*: Within the simulations, cohorts of cells are highlighted (color coded) so that pattern changes can be followed. This marking is passed from parent to daughter cells but has no other effect on the simulations. The only active cell state used in any of the simulations is the binary state of "streak" versus "non-streak". In some simulations (see Sections 2.5 and 2.6 in main text and Figs. 8–10), cells may convert based upon the state composition of the cohort of neighboring cells. Cells determine near - neighborness by a local Delaunay–Voronoi partitioning (O'Rourke, 1998).
- *NUDGE EVENTS*: When a cell changes position or grows it may come into spatial conflict with one or more neighbor cells. The mechanism used to resolve this conflict is termed the *nudge event*. In these simulations, the basic nudge event consists of *direct displacement* (Fig. 12). Neighbors are displaced along a vector defined by a direction running from the center of the new position of the instigating cell to the center of the neighbor and by a magnitude just large enough to eliminate overlap. As neighbors are displaced, they in turn displace their own neighbors. This produces a *ripple* effect which extends outward from the initial cell. In real tissues, where cells are not inelastic spheres, we do not imagine that local alterations in cell geometry or position will have distant effects. However, in a close-packed, or nearly close-packed, collection of spheres movement in any one locale is likely to be transmitted some distance. Two techniques are used in these simulations to prevent cell movement/growth from rippling out to produce distant effects in the tissue. First, the direct displacement vector is enlarged by a small amount (1.0 μm) so that, in general, the tissue is not tightly packed and there is a small amount of space between cells (Fig. 12). This produces some "elasticity", or

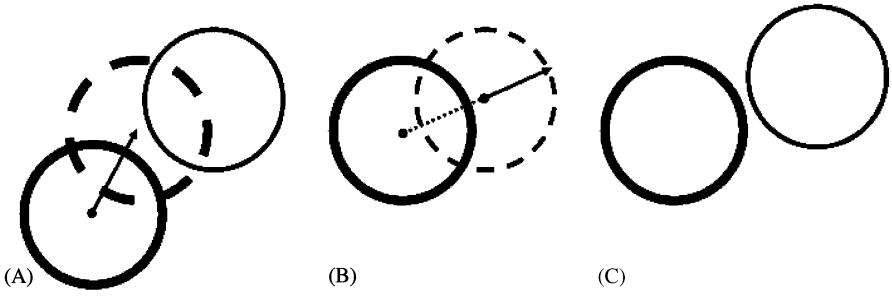

Fig. 12. *Direct displacement* is shown. In (A), a cell (thick solid circle) is moved to a new position (thick dashed circle). This causes spatial conflict with a neighbor (thin solid circle). In (B), the neighbor is directly displaced along a direction vector running from the center of the instigating cell in its new position to the center of the neighbor. In (C), the result is a new position for both cells with no spatial conflict. The displacement includes a small, extra amount to maintain some buffering distance between the cells at completion of the event (see Appendix B text). For illustration, the amount of movement has been exaggerated relative to that in the actual simulations.

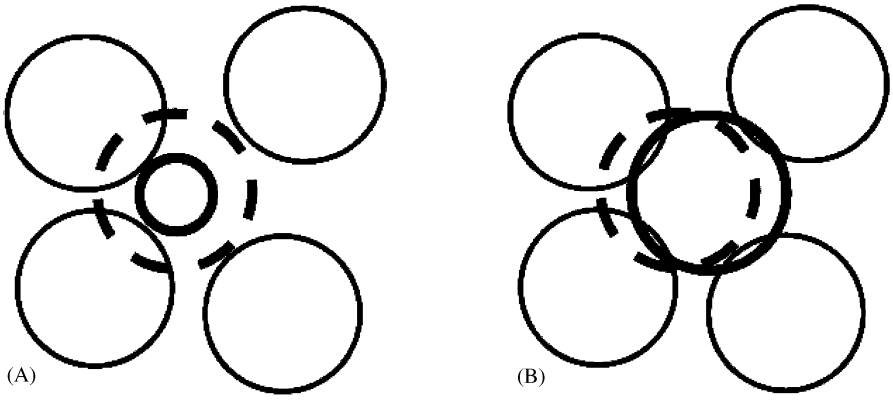

Fig. 13. The *jiggle event* is shown. This event is used to minimize spatial conflicts during cell movement or growth; pictured here is growth. In (A), a cell (thick solid circle) grows (thick dashed circle). This puts it in spatial conflict with two of four neighbors. Elimination of these conflicts by direct displacement (see Fig. 12) would require large movements of two neighbors and no movement of the other two neighbors. Instead, in (B), the instigating cell (thick dashed circle) is displaced slightly (thick solid circle) to minimize the summed spatial conflict with all neighbors. This residual conflict is then resolved by smaller direct displacement of all four neighbors. Depending on the geometry, this jiggle event sometimes eliminates all spatial conflict without the need for any direct displacements. The repositioning of the instigating cell is by iterative, successive approximations.

buffering, in the tissue as a whole to counteract the inelasticity of individual cells. Second, prior to direct displacement of neighbors, the position of the instigating cell is adjusted to minimize the cumulative overlap with its neighbors. This is termed the *jiggle event* (Fig. 13). The first method is applied in all cases. The second is not applied to the active movement of cells but is applied when they grow or are displaced during the nudge event. Simulations in which these techniques are not applied produce comparable results (not shown) but tend to produce slightly more cell mixing (see Discussion).

References

Bachvarova, R.F., Skromme, I., Stern, C.D., 1998. Induction of primitive streak and Hensen's node by the posterior marginal zone in the early chick embryo. Development 125, 3521–3534.

Bellairs, R., 1961. Cell death in chick embryos as studied by electron microscopy. J. Anat. 95, 54–60.

Bodenstein, L., 1986. A dynamic simulation model of tissue growth and cell patterning. Cell Differ 19, 19–33.

Canning, D.R., Amin, T., Richard, E., 2000. Regulation of epiblast cell movements by chondroitin sulfate during gastrulation in the chick. Devel. Dynam. 219, 545–559.

Derrick, G.E., 1937. An analysis of the early development of the chick by means of the mitotic index. J. Morphol. 61, 257–284.

Eyal-Giladi, H., Kochav, S., 1976. From cleavage to primitive streak formation: a complimentary normal table and a new look at the first cleavage stages of the development of the chick. Dev. Biol. 49, 321–337.

Eyal-Giladi, H., Debby, A., Harel, N., 1992. The posterior section of the chick's area pellucida and its involvement in hypoblast and primitive streak formation. Development 116, 819–830.

Foley, A.C., Skromne, I., Stern, C.D., 2000. Reconciling different moels of forebrain induction and patterning: a dual role for the hypoblast. Development 127, 3839–3854.

Gierer, A., Meinhardt, H., 1972. A theory of biological pattern formation. Kybernetik 12, 30–39.

Gräper, L., 1929. Die Primitiventwicklung des Hühnchens nach stereokinematographischen Untersuchungen, knotrolliert durch vitale Farbmarkierung und verglichen mit der Entwicklung anderer Wirbeltiere. Arch. Entw. Mech. 116, 382–429.

Gurdon, J., 1988. A community effect in animal development. Nature 336, 772–774.

Hamburger, V., Hamilton, H.L., 1951. A series of normal stages in the development of the chick embryo. J. Morphol. 88, 49–92.

Hatada, Y., Stern, C.D., 1994. A fate map of the epiblast of the early chich embryo. Development 120, 2879–2889.

Helde, K.A., Wilson, E.T., Cretekos, C.J., Grunwald, D.J., 1994. Contribution of early cells to the fate map of the zebrafish gastrula. Science 265, 517–520.

Ho, R.K., 1992. Cell movements and cell fate during zebrafish gastrulation. Development (Suppl. 1992), 65–73.

Keller, R., 2002. Shaping the vertebrate body plan by polarized embryonic cell movements. Science 298, 1950–1954.

Kelly, K., Wei, Y., Mikawa, T., 2002. Cell death along the embryo midline regulates left-right sidedness. Devel. Dynam. 22, 238–244.

Lawson, A., Schoenwolf, G.C., 2001a. New insights into critical events in avian gastrulation. Anat. Rec. 262, 238–252.

Lawson, A., Schoenwolf, G.C., 2001b. Cell populations and morphogenetic movements underlying formation of the avian primitive streak and organizer. Genesis 29, 188–195.

Levy, V., Khaner, O., 1998. Limited left-right cell migration across the midline of the gastrulating avian embryo. Deve. Genet. 23, 175–184.

O'Rourke, J., 1998. Computational Geometry in C. Cambridge University Press, Cambridge 376pp.

Patten, B.M., 1971. Early Embryology of the Chick. McGraw-Hill Book Company, New York 284pp.

Psychoyos, D., Stern, C.D., 1996. Fates and migratory routes of primitive streak cells in the chick embryo. Development 122, 1523–1534.

Romanoff, A.L., 1960. The Avian Embryo: Structural and Functional Development. The Macmillian Company, New York 1305pp.

Sanders, E.J., Varedi, M., French, A.S., 1993. Cell proliferation in the gastrulating chick embryo: a study using BrdU incorporation and PCNA localization. Development 118, 389–399.

Sanders, E.J., Torkkeli, P.H., French, A.S., 1997. Patterns of cell death during gastrulation in the chick and mouse embryos. Anat. Embryol. 195, 147–154.

Spratt, N.T., 1946. Formation of the primitive streak in the explanted chick blastoderm marked with carbon particles. J. Exptl. Zool. 103, 259–304.

Stern, C.D., 1979. A re-examination of mitotic activity in the early chick embryo. Anat. Embryol. 156, 319–329.

Stern, C.D., 1990. The marginal zone and its contribution to the hypoblast and primitive streak of the chick embryo. Development 109, 667–682.

Stern, C.D., 2004. Gastrulation in the chick. In: Stern, C.D. (Ed.), Gastrulation: from cells to embryo. Cold Spring Harbor Press, Cold Spring Harbor, NY, pp. 219–232.

Stern, C.D., Canning, D.R., 1990. Origin of cells giving rise to mesoderm and endoderm in chick embryo. Nature 343, 273–275.

Stroustrup, B., 1997. The C++ Programming Language, 3rd ed. Addison-Wesley, Reading, MA 911pp.

Waddington, C.H., 1932. Experiments of the development of chick and duck embryos cultivated in vitro. Philos Trans. Roy. Soc. Lond. Ser. B 221, 179–230.

Wei, Y., Mikawa, T., 2000. Formation of the avian primitive streak from spatially restricted blastoderm: evidence for polarized cell division in the elongating streak. Development 127, 87–96.

Wetzel, R., 1929. Untersuchungen am Hühnchen Die Entwicklung des Keims während der ersten beiden Bruttäge. Arch. Entw. Mech. 119, 188–321.

Wilson, E.T., Cretekos, C.J., Helde, K.A., 1995. Cell mixing during early epiboly in the zebrafish embryo. Dev. Genet. 17, 6–15.

Wolpert, L., 1969. Positional information and the spatial pattern of cell differentiation. J. Theor. Biol. 25, 1–47.

Wolpert, L., 1971. Positional information and pattern formation. Curr. Top. Devel. Biol. 6, 183–224.